An easy to build, high intensity monochromator for Helium II radiation applied to inner valence photoelectron studies of small molecules.

by

P. Baltzer, M. Carlsson Göthe, B. Wannberg and L. Karlsson

Department of Physics,
Uppsala University
Box 530, S-751 21 Uppsala
SWEDEN

UUIP 1228 Sep 1990

Abstract

An easy to build, high intensity monochromator for helium II radiation is presented. The design includes a double focusing, non blazed, toroidal grating with a groove density of 800 l/mm. The adjustment and focusing properties of the design have been studied using an optical simulation program. It is found that all necessary adjustments of the grating may be performed by using only two degrees of freedom; rotation and sidewise shifting. Inner and outer valence photoelectron spectra of N_2 and CO have been recorded using monochromatized HeIIα radiation. The study reveals extensive vibrational structures in the inner valence region of both molecules. A new state has been identified in the CO molecule.

INTRODUCTION

During the past year a high intensity 10GHz ECR HeI and HeII line source [1] has been used in photoelectron spectroscopy and ion fragment studies [2]. This source has at least one order of magnitude higher intensity than previously used helium lamps, and is now commercially available. The radiation created in the ECR lamp contains numerous components [1]. Beside the HeI and HeII series, a number of other lines resulting from doubly excited states have been observed [3].

The increase in radiation intensity achieved by this source has made possible investigations of weak structures in the outer valence region using the HeIα line at 21.2 eV and of inner valence structures using the HeIIα line at 40.8 eV. However, studies of the inner valence region have been limited by an intense background resulting from excitation with lines in the HeI series. Practically, the usable energy has ranged from 0 to approximately 26 eV binding energy.

To extend the useful energy range in the recorded spectra the radiation has to be monochromatized, mainly in order to suppress the HeI components. A number of requirements were stated as guidelines in the design of a monochromator.

- Low requirements on energy resolution; (±5 eV).
- Minimal degradation of the HeII intensity.
- High requirements on the suppression of scattered radiation.
- Simple monochromator construction, including mounting, alignment and adjustment.
- Compatible with the existing instrumentation for photoelectron and ion fragment spectroscopy, *e.g.* excitation chamber and VUV lamps.
- Simple reconditioning of the grating.

A new monochromator for HeII has been constructed according to these guidelines. By using a double focusing toroidal grating at low angle of incidence the intensity losses of the HeII radiation is minimized. Ray tracing simulations show that only two degrees of freedom are needed to compensate for manufacturing and mounting errors. The contributions from scattered radiation and from low energy electrons generated wherever the radiation hits a surface have been minimized by a careful design of the regions around the sample gas cell. Performance tests, using the new monochromator, have shown that the useful binding energy region in photoelectron spectra is extended up to 40 eV.

THEORY

All monochromators consist of one or more dispersive elements. In the VUV wavelength region gratings are used. To increase the intensity of the radiation, concave focusing gratings are preferable, compared to planar. To maintain perfect focusing of the object both the image and the object must be positioned along the Rowland circle, *cf* figure 1.

In order to avoid astigmatism, i.e. non-coinciding images in two perpendicular directions, at large angles of incidence and diffraction, a toroidal grating surface , having different radii of curvature in two perpendicular directions has to be used. The radii are chosen to give a stigmatic image at the used angle of incidence and a certain wavelength. The simulations described below show that neither the astigmatism nor the focussing are seriously affected for the present purposes even when the grating is used at the HeIα wavelength although it is optimized for HeIIα.

When designing the monochromator the basic idea was that all necessary monochromator adjustments should be done using only two degrees of freedom; a shift along the x-axis, compensating for imperfections in mounting, and a rotation around the same axis, for wavelength adjustment (*cf* figure 2).

To verify that a sufficiently accurate adjustment may be performed in this manner, simulations were performed using the SHADOW ray tracing program package [4]. The objectives of the simulations were to

- Verify the resolution and focusing of the HeII and HeI radiation.
- Observe the effects of small displacements of the components in the optical system.
- Check the possibility of correcting for displacements using only two degrees of freedom.

The geometry used in the calculations is shown in figure 2. The design of the monochromator allows no adjustment of the source or the image positions relative to the rotational axis of the grating, *cf* figure 3. Therefore, the source and image planes, along with the angle between the incident and reflected ray, were held constant during all simulations. The source object used in the simulations was a 0.5 x 0.5 mm square. Some results of the simulations, referred to as simulation 1 - 6, are presented in Appendix A.

The first two examples demonstrate the resolution and focusing of the HeI and HeII radiations. Four wavelengths were included in the calculations; HeIα, HeIβ, HeIIα and HeIIβ at 584Å, 537Å, 304Å and 256Å, respectively. Simulation plot 1 of Appendix A shows the image obtained from the grating when adjusted for HeIIα radiation. Simulation plot 2 shows the image when the grating is adjusted for HeIα simply by a $\approx 2°$ rotation around the x_G-axis relative to the angle used for HeIIα radiation. Note that the focusing of the HeI components is apparently almost as good as for the HeII components in spite of the off-Rowland circle condition.

Finally, four simulations are shown demonstrating the imaging properties at small manufacturing and mounting errors of the system. These misalignments are represented by displacements of the source along the x_S- and z_S-axes, *cf* figure 2. These shifts of the source correspond to both a shift of the light source and a rotation of the grating around the z_G-axis (introducing a non -perpendicularity of the rulings with respect to the optical axis of the system). The result of the calculations shows that usable monochromatization and focusing is obtained even at a source displacement of 2 mm with respect to the reference point, which is more than any concievable manufacturing or mounting error. The results are shown in simulation plots 3 to 6.

THE MONOCHROMATOR

Based on the criteria and simulations presented above, a new monochromator is presented. The unit is easy to build and is housed in one piece. It interfaces to the instrument and VUV lamps by standard CF35 flanges. Furthermore, the grating alignment and wavelength adjustment are performed using only the two mutually independent degrees of freedom mentioned above. The wavelength is adjusted by a knob with digital scale. Both adjustments are essentially backlash-free.

A toroidal, non blazed, grating manufactured by Astron is used. The grating is optimized for 304 Å, (HeIIα at 303.78 Å). The groove density is 800 l/mm and the depth is 7.6 nm. The ruled area is 20 x 13 mm, and the major and minor radii of curvature are 260.0 mm and 24.5 mm respectively. The initial gold coating was 200 Å thick. The grating is intended to be used with an incidence angle $\alpha = 16°$, and a dispersion angle $\beta = 20°$, with an object distance of 71 mm and an image distance of 90 mm. For HeIIα radiation the dispersion is 6.46 eV/mm at 90 mm object distance.

The upper part of figure 4 shows a schematic drawing of the monochromator. The monochromator house consists mainly of a stainless steel tube with two CF35 flanges welded at 36° angle (*cf* figure 3). The grating is positioned in the center of the lower, horizontal, flange and is held by a frame. The frame may rotate around its shaft. The grating is fastened to the frame by a thin bronze clip.

The desired wavelength is set by tilting the grating. The tilt is actuated by a plunge welded to a bellow feedthrough. The connection is obtained by a screw, pushing the plunge. The vacuum sealing is obtained by the flexible bellow, welded to the plunge and the monochromator house. The bellow, with its atmospheric pressure load, also acts as a spring pulling the arm, thus allowing a backlash-free movement of the plunge. The arm is connected to the grating frame via a thin piece of copper, sliding between two steel balls. The pressure applied to the balls is controlled by a spring and a screw.

As previously mentioned, the wavelength is set using a knob with digital readout. One scale increment (s.i.) in the digital readout corresponds to 1/100 revolution of the screw. The pitch of this screw is 0.7 mm/rev. resulting in a wavelength shift of 2.4 Å/s.i. at 304Å.

The shaft of the frame is held by two hollow screws, and the shifting of the frame is performed by one of these, *cf* lower part of figure 4. The adjustment is completely backlash-free, since a compressed spring in the fixed screw guarantees that the shaft is pushed into the base of the adjustable screw. The screws are sealed by O-rings. When dismounting the monochromator for reconditioning, the grating is removed simply by unscrewing the adjustment screw.

PERFORMANCE TESTS

The monochromator performance has been tested by recording photoelectron spectra of two small molecules; N_2 and CO. To check the radiation components remaining in the HeII region after monochromatizion, a helium photoelectron spectrum was also recorded.

All samples were commercially obtained and run under equivalent experimental conditions. The experiments were performed using a photoelectron spectrometer specialized for gas phase studies [5]. The pressure in the gas cell was held at approximately 20 mTorr.

No impurities were found in the spectra, except helium gas due to an unavoidable leakage from the lamp. One clearly sees the He $1s_{1/2}$ line at 24.587 eV (excited by the 304Å radiation component) in all spectra. This line can be used for calibration purposes.
Considerable work has been done to reduce the background in the recorded spectra. There are two different types of background, one broad and structureless part appearing at kinetic energies below ≈6 eV and one part consisting of lines which are due to ionization by scattered HeI radiation. The scattering is due to imperfections in the coating of the grating and probably also resonance scattering in the He gas. The HeI intensity was reduced by painting illuminated parts of the monochromator (except the grating) with colloidal graphite. The structureless background, which is more or less exponentially increasing towards zero kinetic energy is, at least partly, caused by photoelectrons excited by radiation hitting the metal at the gas cell entrance and exit openings and also at the lens entrance slit. This background has been considerably reduced by screening and by introduction of a series of apertures. Figure 5 shows a schematic drawing of the area around the gas cell. By forming gradually wider apertures, the unwanted illumination may be reduced.

However, the overall background of the recorded spectra is low, generally in the order of $1:10^4$ compared to HeII-excited outer valence lines.

To obtain a high intensity from the monochromator the grating has to be periodically reconditioned. The intensity loss is partly due to tantalum from the ECR microwave lamp, forming an rough layer on the grating. Figure 6 shows the radiation degradation as a function of run time. It was found that recoating is necessary after ≈100 h usage. The grating is reconditioned by dissolving the Au and Ta coating in an Aqua regia, $HNO_3 - HCl$, mixture. The quartz glass is then exposed to a degreasing washing liquid, and finally cleaned in distilled water. A new Au layer is then sputtered to the grating, using a commercial sputtering device from Balzers. A layer thickness of approximately 200Å was used in the present studies.

The reflected radiation from a grating can be expected to be to some extent polarised. To check the degree of polarisation, spectra of CO_2 were taken with the grating lines parallel and perpendicular to the direction of the photoelectrons. The anisotropy of photoelectrons from CO_2 has been measured earlier at both the HeI and HeII wavelengths [6]. The large differences in anisotropy between the close-lying A - and B-states at both wavelengths make this molecule well suited for calibration of the polarisation. For HeI radiation, the data indicate a polarisation of about 30%, while the polarisation for HeII is less than 10%.

Since the primary purpose of the monochromator is to suppress the intense HeI radiation while maintaining as high HeII intensity as possible, its energy resolution as defined by source size and image slit is not high. Measurement of the line profiles show that the FWHM at the HeIIα line is about 10 eV. Consequently, a number of helium radiation components, of low intensity compared to the HeIIα line, fall withing the energy window defined by the monochromator and give rise to weak satellite structures in the spectra. One may note that even the HeIIβ line falls more or less within this energy region.

Although the grating is optimized for HeIIα, the focusing is good also for HeIIβ, as discussed in the previous section. Therefore, due to the high intensity of the ECR source, studies may be performed using also monochromatized HeIIβ radiation for excitation.

To check the relative intensities of the He radiation components present in the energy region of interest with the grating adjusted for HeIIα, a photoelectron spectrum of helium was recorded, *cf* Figure 7. The sample pressure was 20mTorr and the recording time was approximately 20 hours. Table 1 summarizes the energies and relative intensities of the helium lines observed in this study.

To aid in the analysis of spectra, a spreadsheet template in Microsoft Excel for the Macintosh has been developed. The spreadsheet takes a HeIIα excited line and calculates the expected photoelectron energies and approximate intensities resulting from excitation of this level with all other He radiation components. Alternatively, one can for a weak unidentified line get a list of possible positions for the corresponding HeIIα-excited line, on the assumption that the unidentified line is excited by some other He radiation component. The use of this spreadsheet template, in combination with a pre-analysis program called CrunchViewer [7], facilitates the analysis of superimposed spectra, arising due to satellite components in the ionizing radiation.

The N_2 molecule

The N_2 photoelectron spectrum has previously been studied extensively. Outer valence spectra have recently been recorded in performance tests of the ECR lamp [1] using HeIIα and HeIIβ radiation. A high resolution HeII excited inner valence spectrum has been published by Åsbrink *et al* [8]. This spectrum shows the C $^2\Sigma^+_u$ state, centred at 25.5 eV, with a well defined vibrational progression up to v=17. Above 28 eV the spectrum gives no useful information due to an intense HeI excited background.

In the present study, we have recorded an outer and inner valence spectrum using monochromatized HeIIα radiation. This spectrum is displayed in figure 8 and shows the transitions to the X-, A-, B-, C-, D-, and E-states of the cation using the assignments made in ref. [9]. In this spectrum the vibrational progression of the C state may be followed up to v=21. The band corresponding to transitions to the D $^2\Sigma^+_g$ state, at 29.2 eV, is found to be structureless, which may suggest that the state is dissociative. The band representing the E $^2\Pi_u$ state, at 31.9 eV, shows a short progression with five vibrational components from the low binding energy part. The vibrational spacings are only slightly converging up to the point where the lines disappear. This may indicate that the state is pre-dissociative due to a potential curve crossing with a repulsive state. In the spectrum of figure 8 one clearly sees the excitations of the X-state in N_2 in the 32 to 34 eV energy region due to scattered HeIα, β, γ and δ radiation. The recording time of the spectrum was 4h30min using a newly recoated grating.

A full report on the study of the N_2 molecule will be published elsewhere [10].

The CO molecule

The high resolution HeII excited photoelectron spectrum of CO has earlier been studied by Åsbrink *et al* [11] and Potts and Williams [12]. In there spectra the inner valence region, starting with the D $^2\Pi$ state at 22.7 eV and the C $^2\Sigma^+$ state at 23.4 eV, shows extensive vibrational structure. However, the seventh state observed at 27-28 eV and assigned as F $^2\Sigma^+$ in ref. [11], is most uncertain due to an exponentially increasing HeI induced background.

In the present study, a new outer and inner valence photoelectron spectrum of CO has been recorded using monochromatized HeIIα radiation. This spectrum, displayed in figure 9, show nine resolved bands with binding energies below 33 eV. The D $^2\Pi$ state observed at 22.9 eV, the C $^2\Sigma^-$ state at 23.4 eV and the E $^2\Sigma^+$ state at 25.3 eV (vertical transitions) correspond well to the results of Åsbrink *et al* [11] as well as Potts and

Williams [12]. The D-, C-, and E-states are obviously all bound or quasi-bound with long vibrational progressions. In the study of Åsbrink *et al*, the next band was observed at 27-28 eV and was associated with transitions to the F $^2\Sigma^+$ state. The present spectrum obtained by monochromatized HeIIα radiation clearly shows that there are two states in this region, the bands centred at 27.5 eV and 28.25 eV. The first band, which we assign as transitions to the F $^2\Sigma^+$ state, is structureless and thus probably dissociative. The second band assigned as the G state shows a vibrational progression with at least five components.

Finally, the band centred at 31.9 eV is found to be essentially structureless. The band is partly overlapped by the HeIα,β,γ,δ progression in the X Σ^+ state. However, these lines do not influence the shape of the band substantially. The recording time of the spectrum was 22 hours. The fairly long run-time was due to low HeII intensity resulting from Ta contamination on the grating.

A full report on the CO molecule will be published elsewhere [10].

CONCLUSIONS

The results presented above show that the simple monochromator presented above gives sufficient reduction in intensity of the HeI components to make possible high resolution inner valence studies using monochromatized HeII for a large number of atoms and molecules.

REFERENCES

[1] P. Baltzer and L. Karlsson, Uppsala University Institute of Physics Report, UUIP-1211, 1989.

[2] P. Baltzer, *Instrumental developments and applications in VUV and low energy charged particle spectroscopy,* Acta Universitatis Upsaliensis 197, Thesis, 1989.

[3] P. Baltzer and L. Karlsson, Phys. Rev. A **38**, 2322 (1988).

[4] F. Cerrina, University of Wisconsin Report, 1987.

[5] P. Baltzer, B. Wannberg and M. Carlsson Göthe, Accepted for publ. in Rev. Sci. Instr., 1990.

[6] H. Veenhuizen, B.Wannberg, L. Mattsson, K.-E. Norell, C. Nohre, L. Karlsson and K. Siegbahn, J. Electron Spectrosc. Relat. Phenom. **41**, 205 (1986)

[7] M. Carlsson-Göthe, L. Karlsson, S. Svensson and J. de Sousa Pires. Submitted to Computers in Physics, 1990.

[8] L. Åsbrink and C. Fridh, Phys. Scr. **9**, 338 (1974).

[9] S. Svensson, A. Nilsson, L. Karlsson, N. Mårtensson and U. Gelius, Uppsala University Institute of Physics Report, UUIP-1200, 1989.

[10] M. Carlsson Göthe, P. Baltzer, B. Wannberg, L. Karlsson and S. Svensson, to be published.

[11] L. Åsbrink, C. Fridh, E. Lindholm and K. Codling. Phys. Scr. **10**, 183 (1974).

[12] A.W. Potts and T.A. Williams, J. Electron Spectrosc. **3**, 3 (1974).

TABLE 1

A summary of the helium lines in the HeIIα range present in the excitation radiation after monochromatization.

Wavelength (Å)	Energy (eV)	Designation	Relative peak hights	Comment
256.32	48,372	HeIIβ	0.032	Usable for spectroscopy.
294.11	42.156	HeI line	0.00047	
295.22	41.998	HeI line	0.00033	
300.6 [a]	41.33	HeI line	0.00029	
303.78	40.814	HeIIα	1.0	Usable for spectroscopy.
305.76	40.550	HeI line	-	
309.1 [b]	40.117	HeI line	0.00065	
320.29	38.710	HeI line	0.0037	

a Average of two lines at 300.49Å and 300.75Å [3].
b Average of two lines at 308.96Å and 309.09Å [3].

Figure captions.

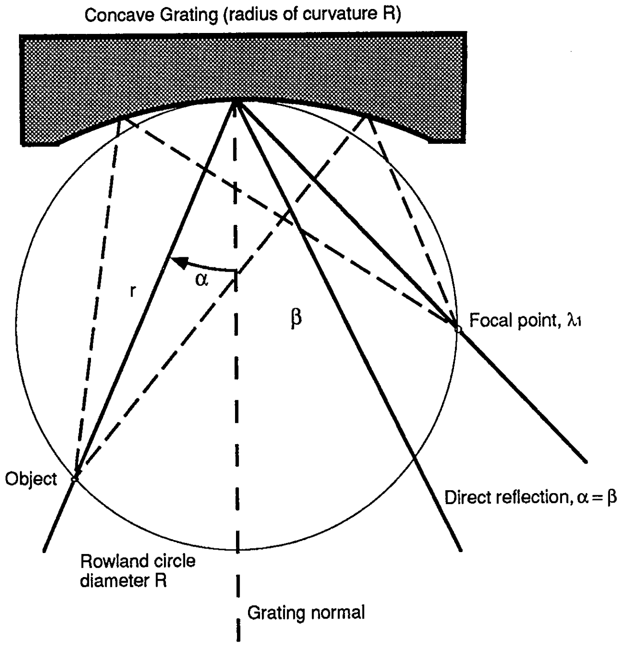

Fig.1. *Schematic drawing of a concave grating with the image and object positioned along the Rowland circle.*

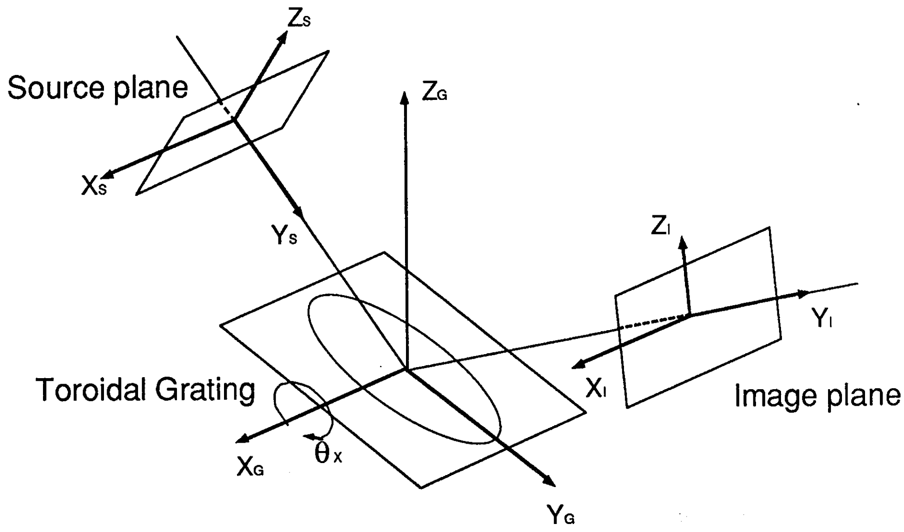

Fig.2. *The source, grating, and image coordinate systems defining the geometry of the monochromator optical system.*

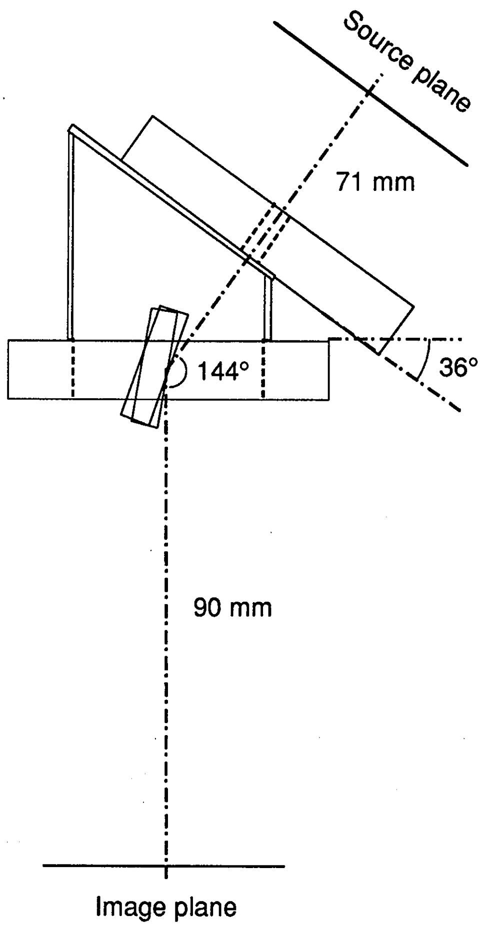

Fig.3. *A simplified drawing of the monochromator housing including the angles and distances of the optical system. Note that the angle between the incident and reflected rays is fixed to 144°.*

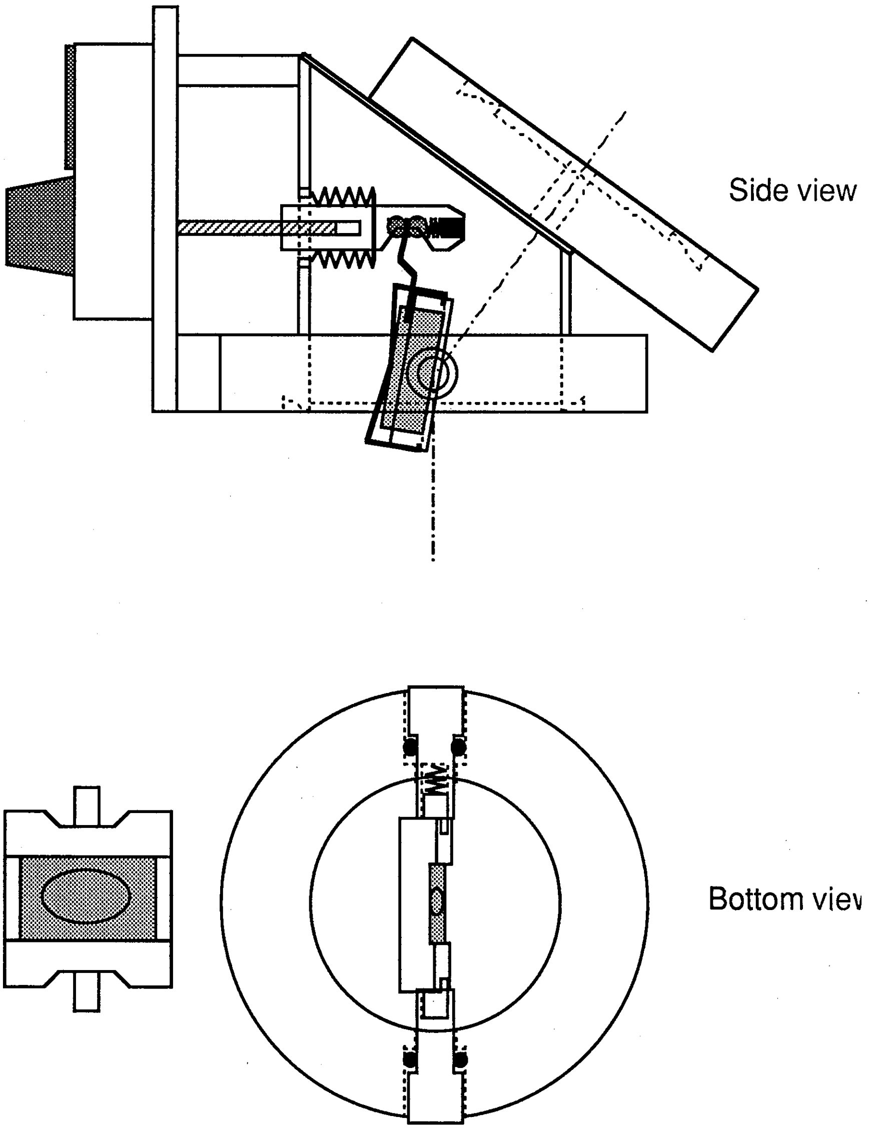

Fig.4. *A schematic drawing showing the design of the monochromator. The grating is held by a stainless steel frame and fastened by a bronze clip. The tilt angle is determined by a bellow system. The grating may be shifted sideways by a screw as shown in the bottom view.*

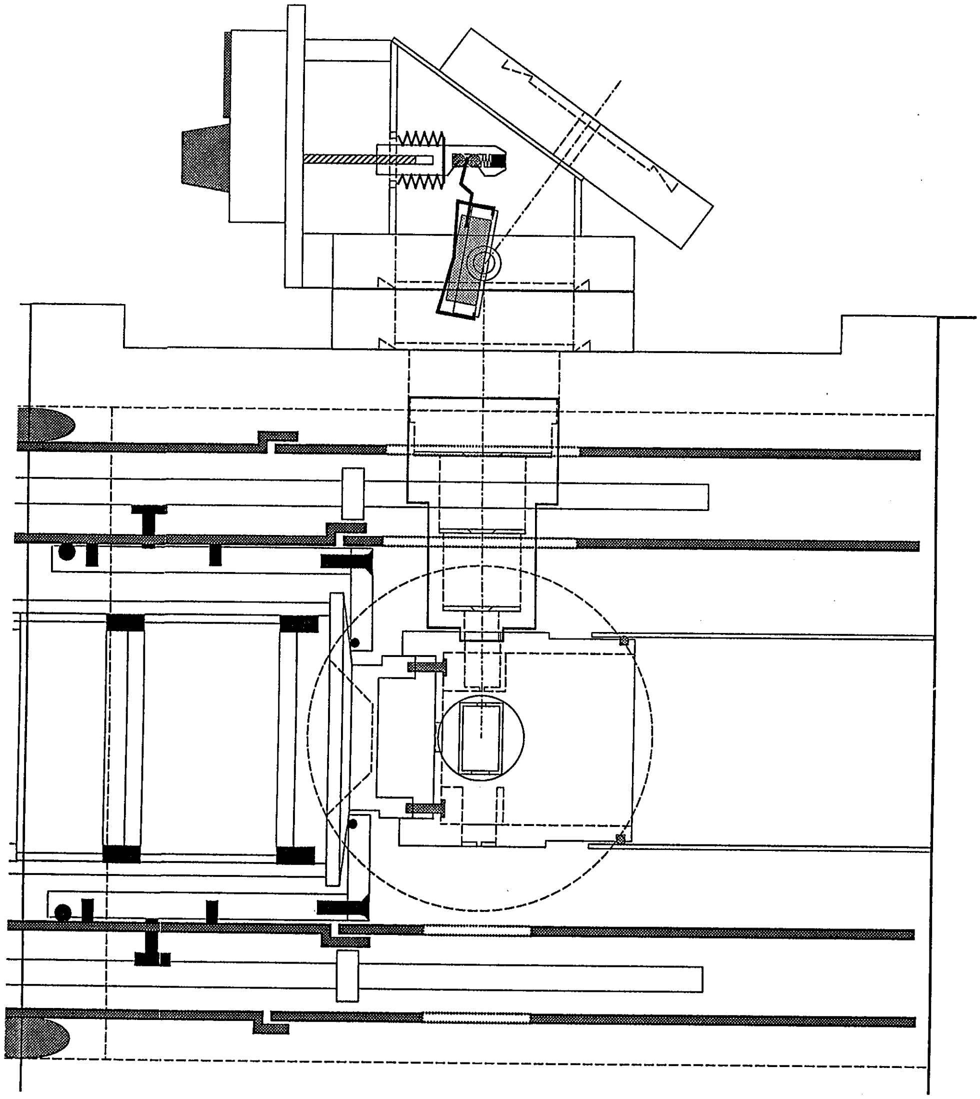

Fig.5. *A schematic overview of the source and excitation compartments of the spectrometer. The figure includes the electron lens, gas cell and screening arangement used to reduce the illumination of the lens slit by scattered light. The magnetic screening is accomplished by μ-metal shields indicated as thick solid lines in the figure.*

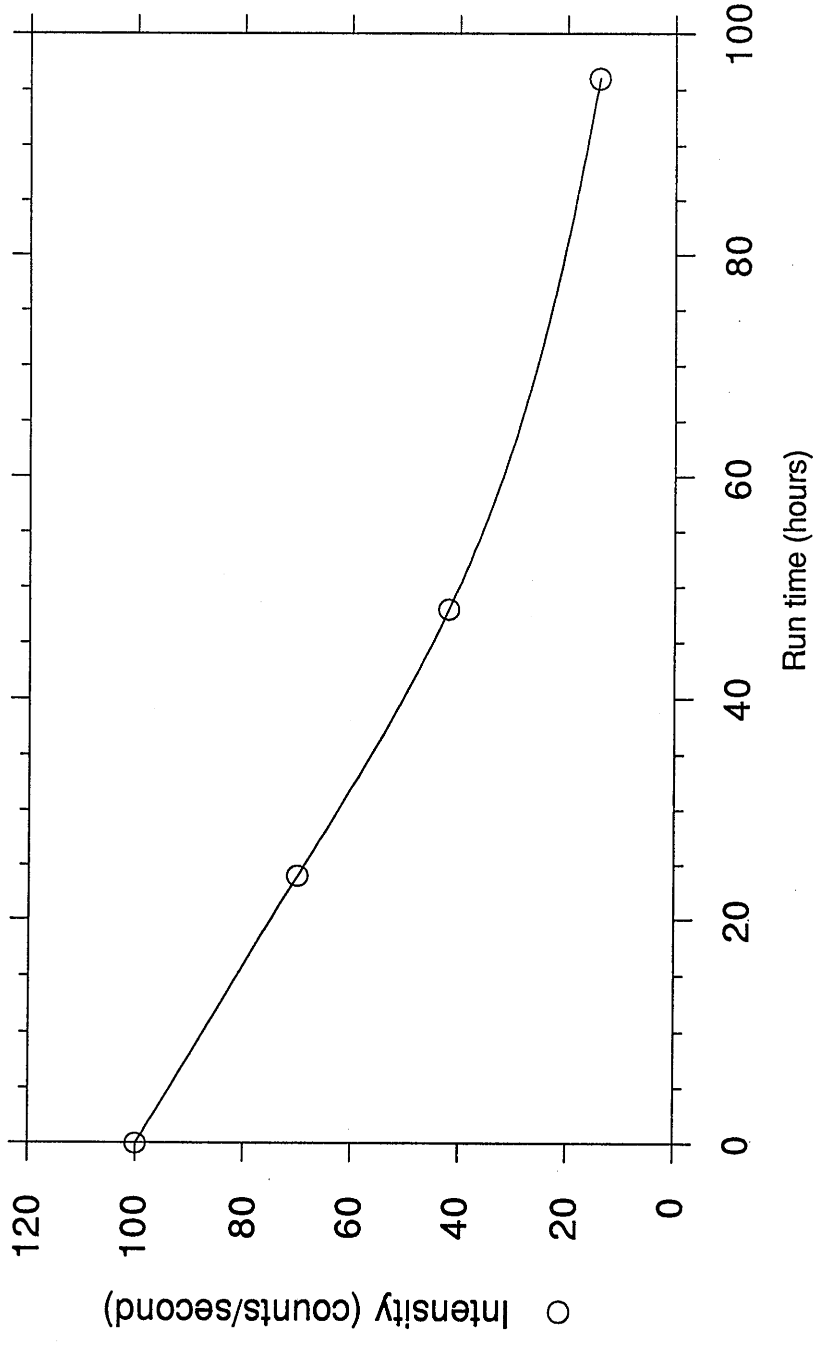

Fig.6. *Reflectivity degradation of the grating surface due to tantalum contamination.*

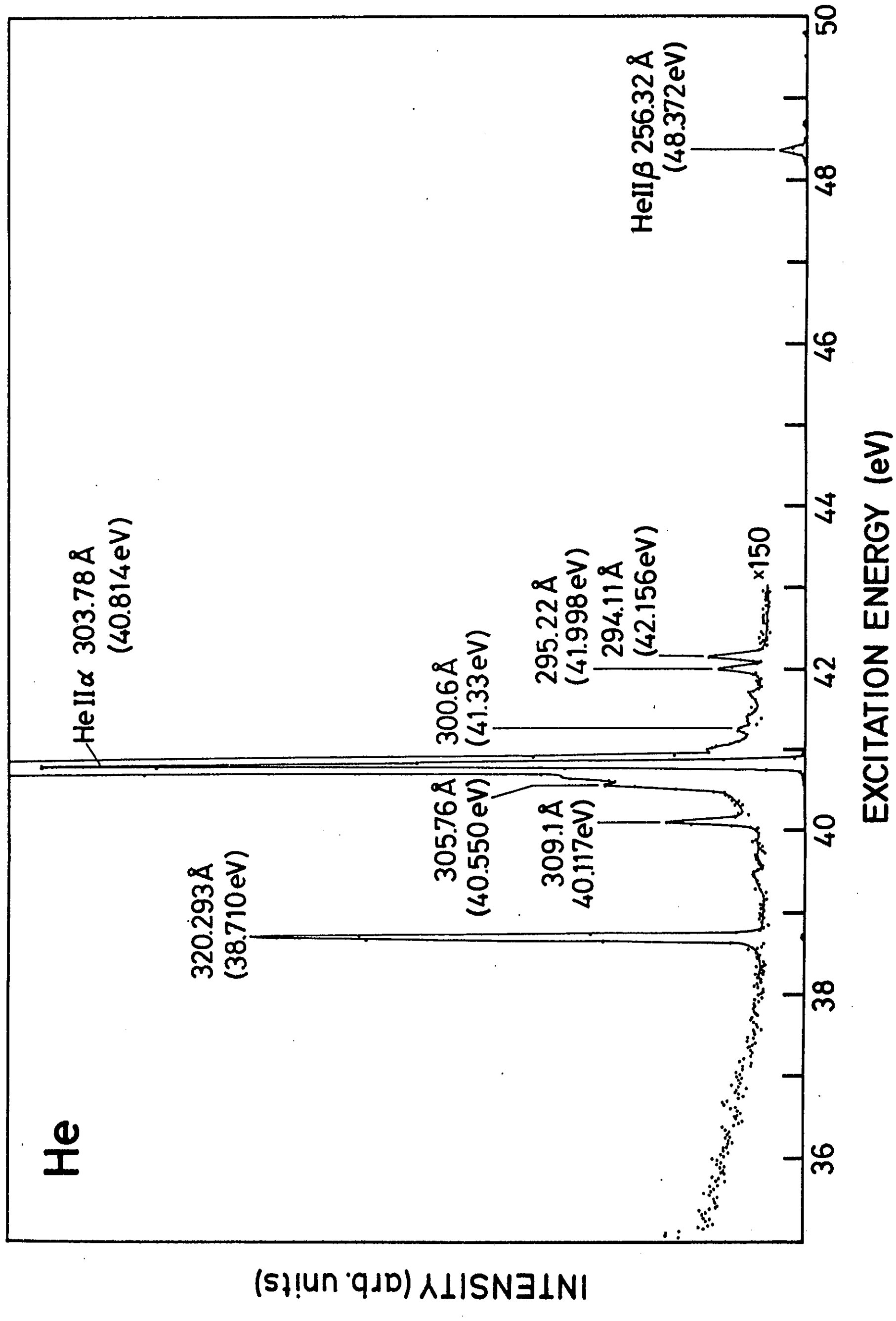

Fig.7. *A photoelectron spectrum of helium showing ionization with different radiation components in the energy region between 35 and 50 eV. The spectrum was recorded using the monochromator.*

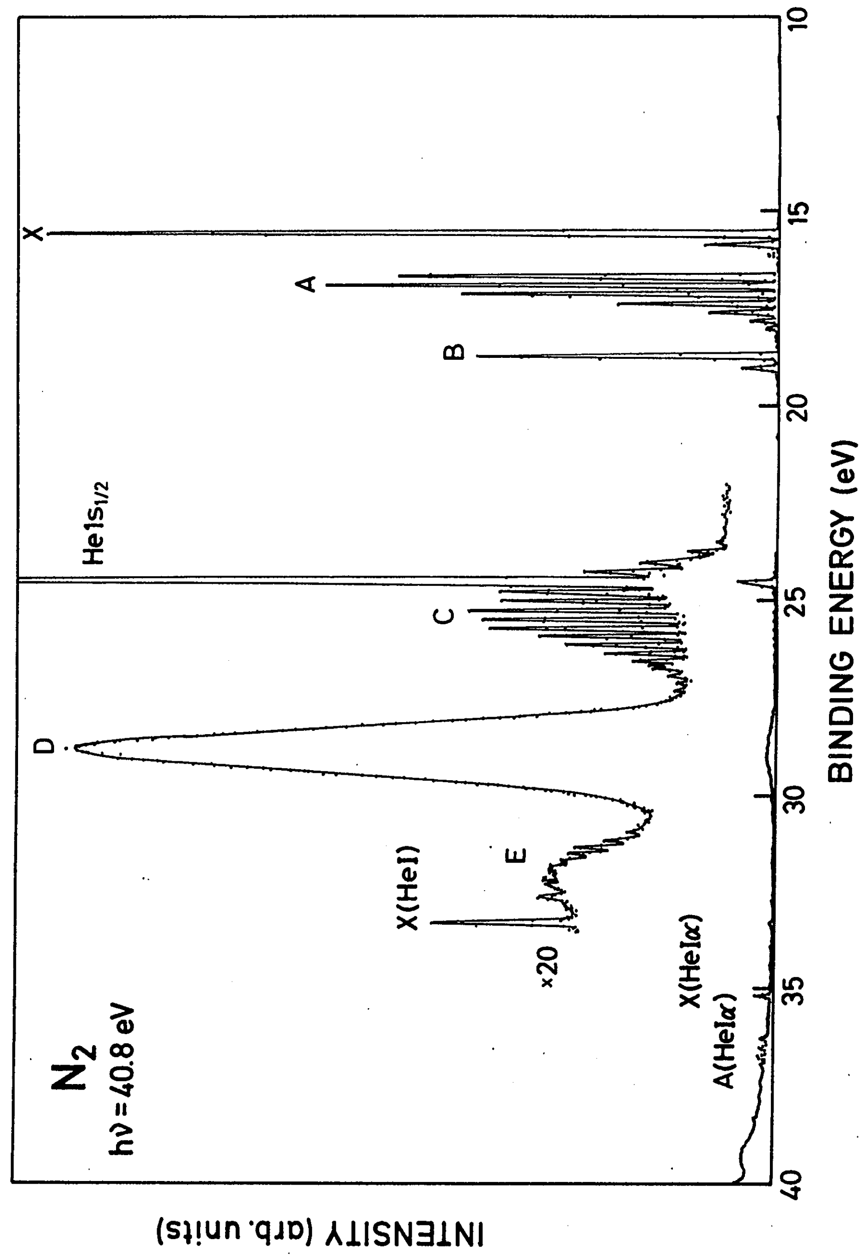

Fig.8. *A photoelectron spectrum of the valence region of N_2 obtained using monochromatized HeIIα radiation. The weak lines above 35 eV are due to ionization with scattered HeIα radiation. The narrow lines superimposed on the band representing the E state at 32 eV are due to ionization from the $3\sigma_g$ orbital with higher components of the HeI radiation.*

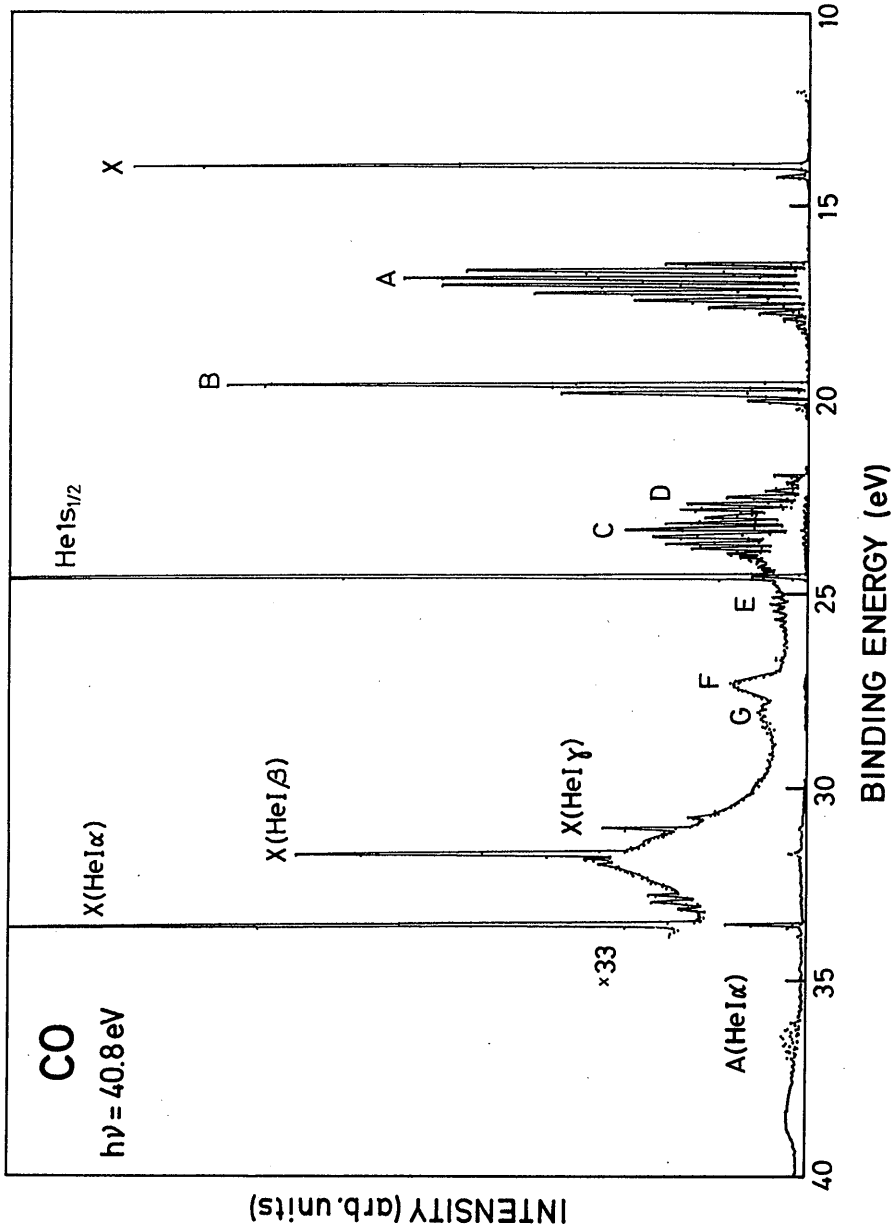

Fig.9. *A photoelectron spectrum of the valence region of CO using monochromatized HeIIα radiation. The weak lines above 33 eV are due to ionization with scattered HeI radiation. The narrow lines superimposed on the band centred at 32 eV are due to ionization from the 5σ orbital with higher components of the HeI radiation.*

Appendix A

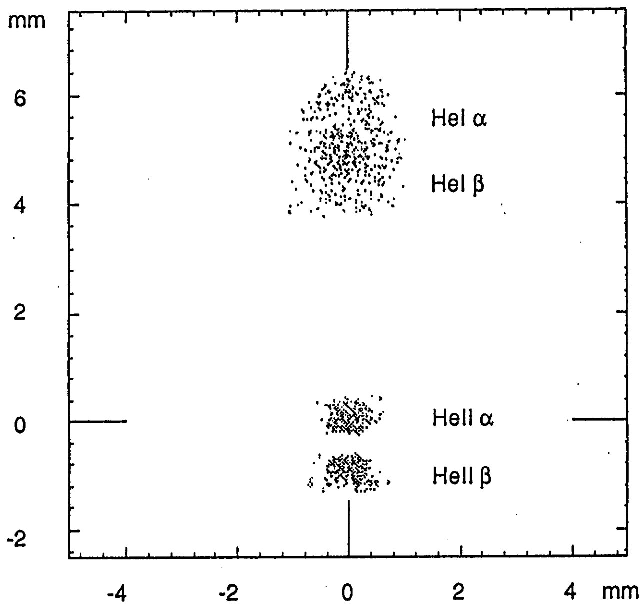

Simulation 1.

Grating adjusted for optimal focusing on HeIIα radiation. The source and image planes, along with the angle between the incident and reflected ray is held constant at 144° during all simulations.

Source plane distance :	71 mm
Image plane distance :	90 mm
Incidence angle :	74.25°
Reflection angle :	69.75°

The raytracing plots show the image, on the image plane, of a 0.5 x 0.5 mm source object. The origin of the image plane is set to correspond to the focal point of the HeIIα radiation.

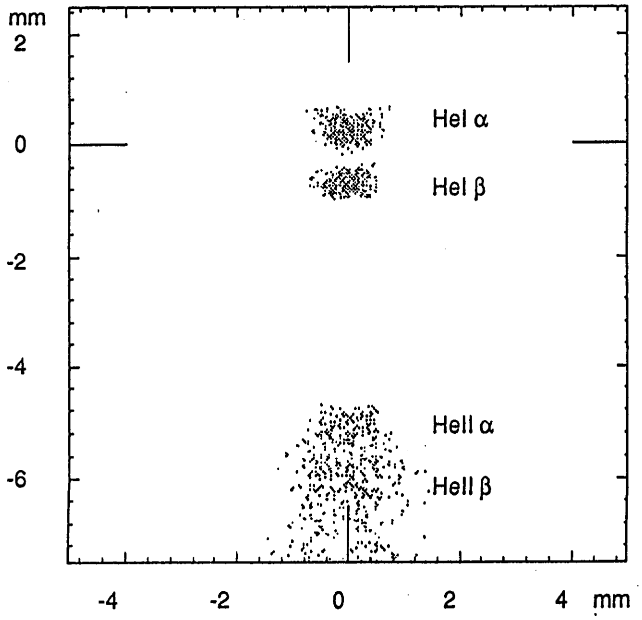

Simulation 2.

Grating adjusted by rotation around the x-axis for HeIα.

The grating is only adjustable in two degrees of freedom, a shift along the x_o-axis and a rotation around the x_o-axis, θ_x, *cf* figure 2 and 3.

$x_o = 0.0$ mm
$\theta_x = 2.0°$

Note, that the focusing of the HeI components is, almost, as good as for the HeII components.

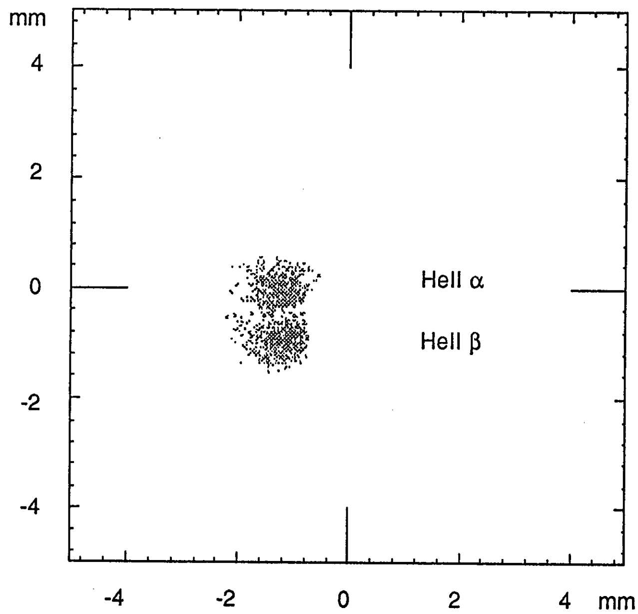

Simulation 3a.

Displacement test.

The source is displaced by a shift in the x_s direction on the source plane. Such a shift is also equivalent with a rotation of the grating around its normal, the z_G-axis.

$x_s = 1.0$ mm
$z_s = 0.0$ mm

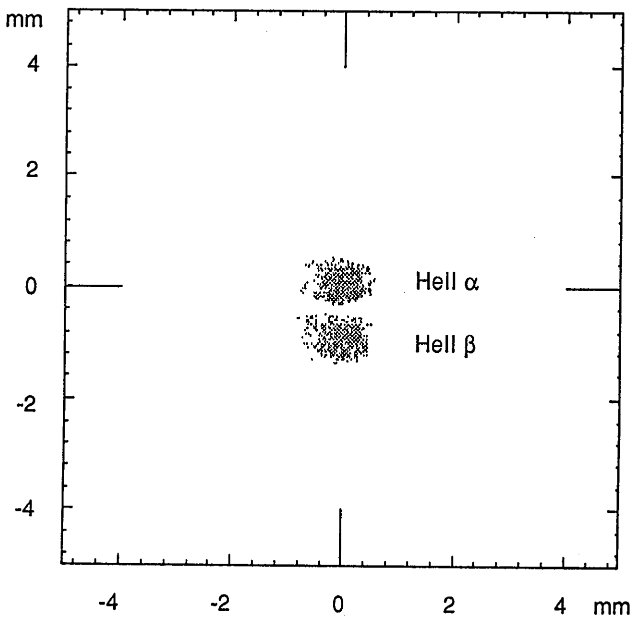

Simulation 3b.

The displacement of the source is compensated for by shifting the grating along the x_G-axis. The adjustment has only a slight effect on the focussing.

$x_G = 0.55$ mm
$\theta_x = 0.0°$

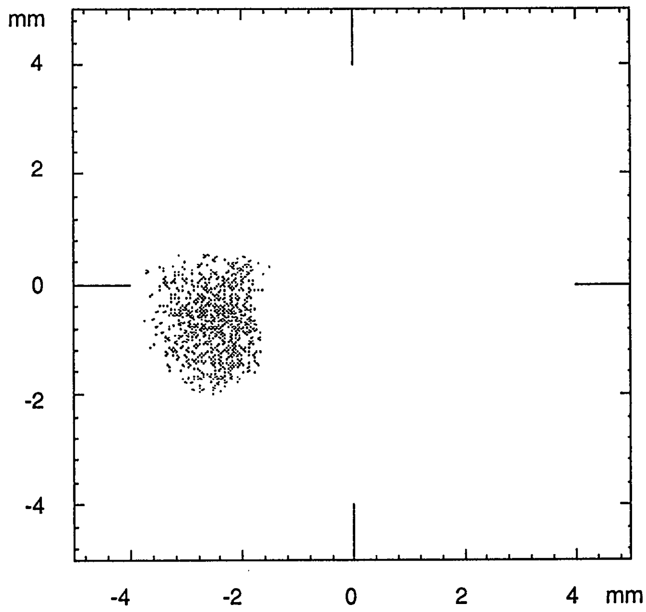

Simulation 4a.

Similar displacement as in sim. 3a but with larger magnitude.

$x_s = 2.0$ mm
$z_s = 0.0$ mm

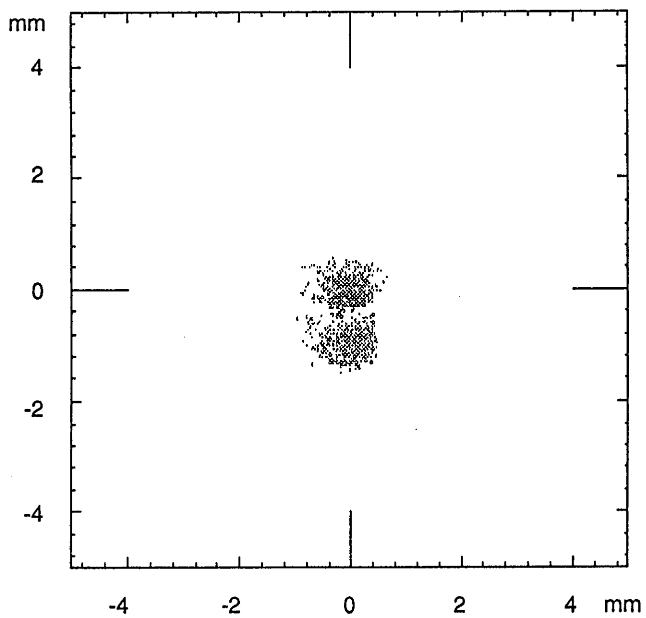

Simulation 4b.

$x_o = 1.10$ mm
$\theta_x = 0.0°$

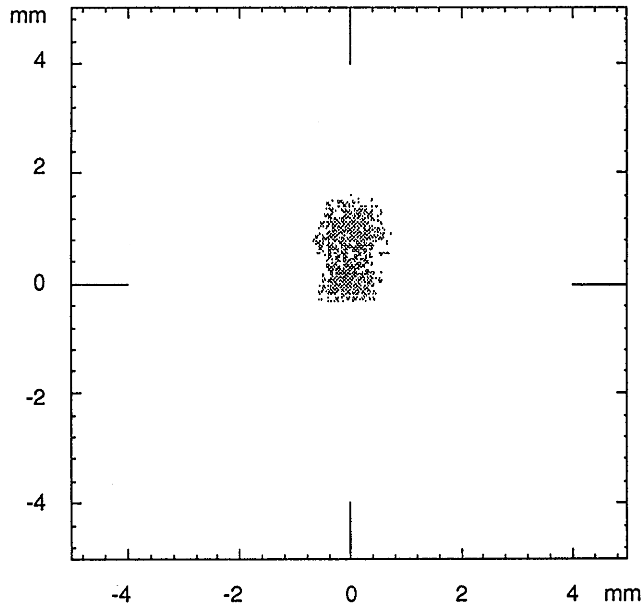

Simulation 5a.

The source is displaced by a shift along the z_s-axis.

$x_s = 0.0$ mm
$z_s = 1.0$ mm

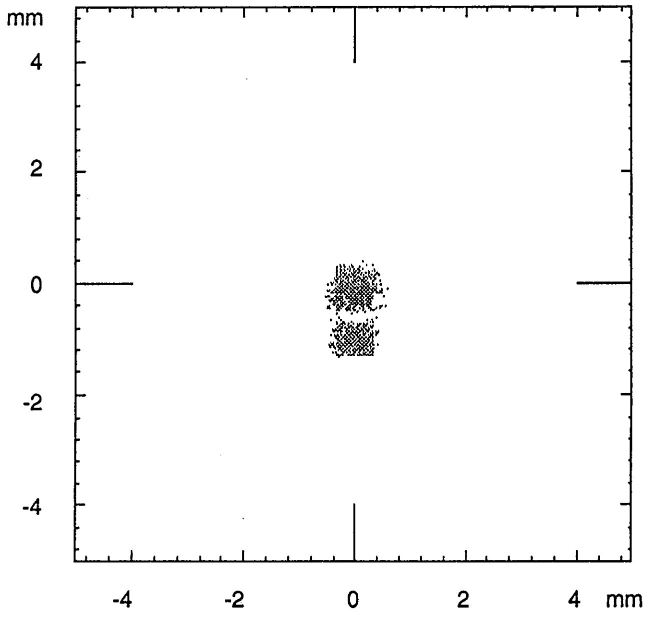

Simulation 5b.

The displacement is compensated for by a rotation of the grating. A compensating rotation of the grating, i.e. a small wavelength adjustment.

$x_o = 0.0$ mm

$\theta_x = 0.4°$

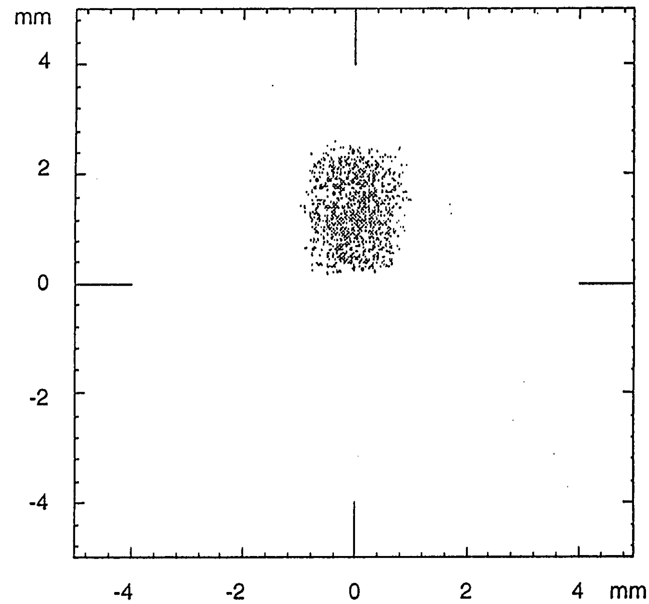

Simulation 6a.

Similar displacement as in 5a, but with larger magnitude.

$x_s = 0.0$ mm
$z_s = 2.0$ mm

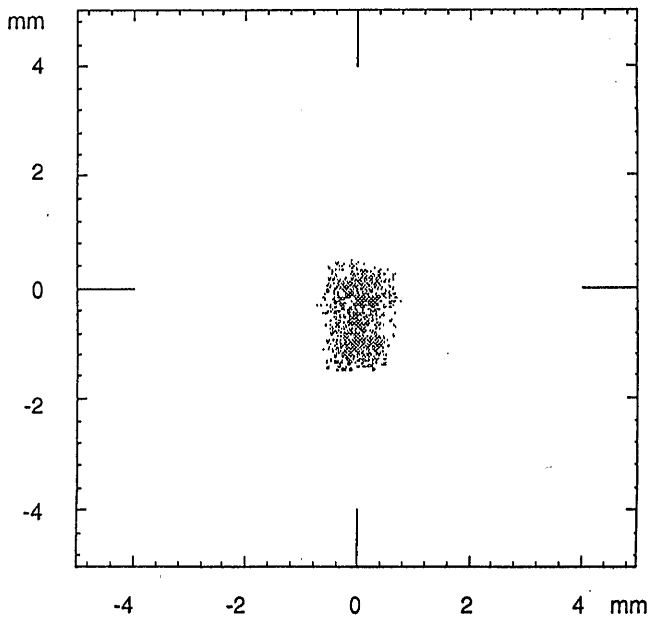

Simulation 6b.

$x_o = 0.0$ mm
$\theta_x = 0.7°$